

Direct numerical simulation of the very large anisotropic scales in a turbulent channel

Juan C. del Álamo* Javier Jiménez†

February 26, 2022

1 Introduction

Over the last decades the knowledge on the small scales of turbulent wall flows has experienced a significant advance, especially in the near-wall region where the highest production of turbulent energy and the maximum turbulence intensity occur. The development of computers has played an important role in this progress, making direct numerical simulations affordable (Kim, Moin & Moser, 1987), and offering wider observational possibilities than most laboratory experiments.

The large scales have received less attention, and it has not been until recently that their significance and their real size have been widely recognized, thanks in part to the experiments by [Hites (1997)] and [Kim & Adrian (1999)], and to the compilation of experimental and numerical data by [Jiménez (1998)]. Two are the main reasons for this. In the first place, when [Townsend (1976)] originally proposed the existence of very large anisotropic scales (VLAS) in the overlap layer under the ‘attached eddy’ hypothesis, he described them as ‘inactive’, not containing Reynolds stresses. [Perry, Henbest & Chong (1986)] repeated that assertion in their elaboration of Townsend’s model, and this has probably contributed to their relative neglect by later investigators. [Jiménez (1998)] showed however that this characterization is only partly correct, and that the VLAS carry a substantial fraction of the Reynolds stresses. We will provide in this report further evidence that they carry a substantial part of the turbulent energy in the flow and that they are ‘active’ in Townsend’s sense.

The large size of these scales also makes them difficult to study, both experimentally and numerically. Many of the high-Reynolds number laboratory experiments lack spectral information, have too few wall distances, or have data records which are too short to capture the largest scales. Moreover, most of them contain only streamwise information, and data on the spanwise scales are scarce. The requirements of both a very large box and a high Reynolds number

*School of Aeronautics UPM, 28040 Madrid, Spain

†Also at School of Aeronautics UPM, 28040 Madrid, Spain

	Re_τ	Δx^+	Δz^+	Δy_{max}^+	L_x/h	L_z/h	N_x	N_z	N_y	Numerics
Moser <i>et al.</i> (1999)	590	7.2	3.6	7.2	2π	π	512	512	257	Spectral
Abe <i>et al.</i> (2001)	640	8.0	5.0	8.2	6.4	2	512	256	256	Second order FD
Present case 1	550	8.9	4.5	6.7	8π	4π	1536	1536	257	Spectral
Present case 2	180	8.9	4.5	6.1	12π	4π	768	512	97	Spectral

Table 1: Summary of cases. The resolution is measured in collocation points

has made direct numerical simulation of the VLAS unapproachable until today. Previously available numerical databases were restricted to low Reynolds numbers, with little or no separation between the small and large scales (Kim, Moin & Moser, 1987), or to small computational boxes which interfere with the VLAS (Moser, Kim & Mansour, 1999; Abe, Kawamura & Matsuo, 2001).

The purpose of this report is to serve as a preliminary description of a newly compiled numerical database of the characteristics of the large scales in turbulent channel flow at moderate Reynolds numbers.

2 The numerical experiment

Our investigation has been carried on a direct numerical simulation of the turbulent incompressible flow in plane channels at Reynolds numbers $Re_\tau = 180$ and $Re_\tau = 550$, based on the wall friction velocity, u_τ , and on the channel half-width h . The emphasis in this report will be on the latter of those two simulations. The numerical code is fully spectral, using dealiased Fourier expansions in the streamwise and spanwise directions, and Chebychev polynomials in the wall-normal one, as in [Kim, Moin & Moser (1987)]. Although there are computations in the literature at somewhat higher, although comparable, Reynolds numbers (Moser, Kim & Mansour, 1999; Abe, Kawamura & Matsuo, 2001; see table 1), we believe that this is the first simulation in which the numerical box is large enough not to interfere with the largest structures in the flow.

The experimental results for high-Reynolds number turbulent wall flows (see the references given in the previous section) reveal that the premultiplied one-dimensional streamwise velocity spectrum $k_x E_{uu}^{1D}(k_x, y)$ has two peaks. The first one is in the wall region and scales in wall units. Its position does not vary with the distance y to the wall and corresponds to the size of the buffer layer streaks. At the top of the buffer layer, the first peak coexists with a second one which scales in outer units and is characteristic of the outer region. The second peak becomes stronger as the Reynolds number increases and its position corresponds to the VLAS. Its length increases with y and reaches a maximum of $4 - 15 \delta$ (where δ is the characteristic flow thickness) at a wall distance which scales in outer units and which depends on the type of flow. Beyond that level, the peak moves to shorter wavelengths, until the streamwise turbulent energy becomes associated to scales of length $\lambda_x \approx \delta$ at $y = \delta$. With this information in mind,

and with the aid of tests cases performed at $Re_\tau = 180$ and $Re_\tau = 550$ in boxes of different sizes, we have used a box of size $L_x \times L_y \times L_z = 8\pi h \times 2h \times 4\pi h$ in the streamwise, wall-normal and spanwise directions for our $Re_\tau = 550$ simulation.

The longest scales in the numerical channels occur in the streamwise velocity u at $y \approx 0.5h$. Fig. 1(a) displays the premultiplied one-dimensional spectra $k_x E_{uu}^{1D}(k_x)$ at that level. It is clear that the most energetic structures have lengths of $2 - 5h$, which are represented by the Fourier modes 5 – 12 in our simulation at $Re_\tau = 550$, and 7 – 18 in the one at $Re_\tau = 180$. The dynamics of the first few Fourier modes are affected by the periodicity of the box, essentially because their resolution in wavelength space is too coarse to provide a healthy interaction amongst the different length scales. The even-odd structure of the long-wave end of the 1 – D spectrum at $Re_\tau = 550$ in Fig. 1(a) is probably due to this effect. It also appears at other wall distances, and has been observed in numerical channels performed with completely different numerics (Guglielmo Scovazzi, private communication).

The widest scales appear at the center of the channel in the spanwise velocity w , whose transverse one-dimensional spectra $k_z E_{ww}^{1D}(k_z)$ have been represented in Fig. 1(b). In this case the peaks of the spectra are sharper than those in Fig. 1(a). Thus, although the most energetic structures are again associated to low Fourier modes (6 – 13 at $Re_\tau = 550$ and 5 – 9 at $Re_\tau = 180$), there is relatively less energy in the poorly-represented modes than in the streamwise direction.

A more quantitative check of the adequacy of the numerical box is to calculate the fractions Φ_u^x and Φ_w^z respectively of the streamwise energy $\langle u'^2 \rangle$ contained in the Fourier modes $k_x = 0, k_z \neq 0$, and of the spanwise energy $\langle w'^2 \rangle$ contained in the Fourier modes $k_x \neq 0, k_z = 0$. These ratios give an idea of how much turbulent energy is contained in fluctuations which are longer or wider than the numerical box, and which are treated numerically as if they were *uniform* in x or z . In Fig. 2(a) we represent Φ_u^x and Φ_w^z from our DNS at $Re_\tau = 550$ and from [Moser, Kim & Mansour (1999)]. Note that in the latter, with $L_x \times L_z = 2\pi h \times \pi h$, roughly 20% of the energy of u is contained in structures which are longer than the numerical box, and that the behavior of w in z is even worse in the outer region, where 30% of its energy is unresolved. From these data we conclude that the box of that simulation is too small to represent the largest flow structures, and that even the present one is in some ways marginal. It should however be noted that numerical experiments at $Re_\tau = 180$ in a shorter box with $L_x = 8\pi$, instead of 12π , showed very little degradation in the resolved part of the longitudinal spectra. On the other hand, low resolution experiments in a box of length $L_x = 6\pi$ at the higher Reynolds number showed signs of contamination of the spectral peak by the numerical effects mentioned above for the long spectral modes.

The grid resolution, given in table 1, is intermediate between those used by [Moser, Kim & Mansour (1999)] for their cases $Re_\tau = 180$ and $Re_\tau = 590$, and is slightly marginal for the smallest scales, specially in the x direction. The result is a spurious accumulation of enstrophy in the short-wavelength tails of the spectra of the velocity derivatives, where they are improperly represented. The most underresolved derivatives are $\partial_x v$ in x and $\partial_z u$ in z . Fig. 2(b) displays

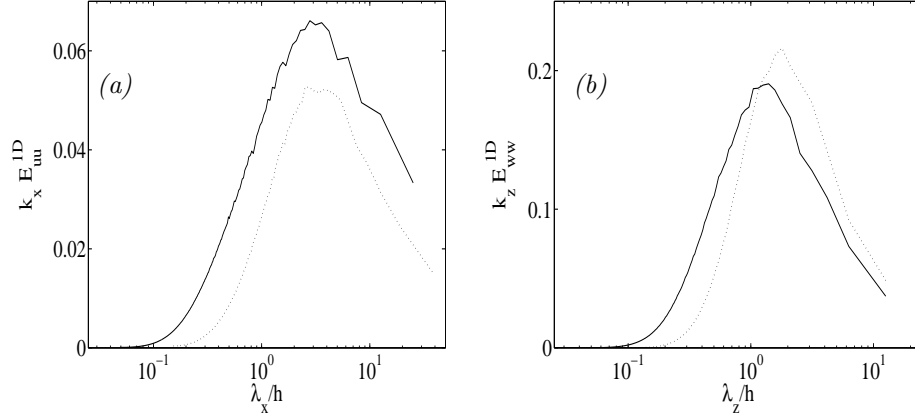


Figure 1: Premultiplied one-dimensional spectra at $y = 0.5h$. —, present $Re_\tau = 550$; ·····, present $Re_\tau = 180$. (a) $k_x E_{uu}^{1D}(k_x)$. (b) $k_z E_{ww}^{1D}(k_z)$;

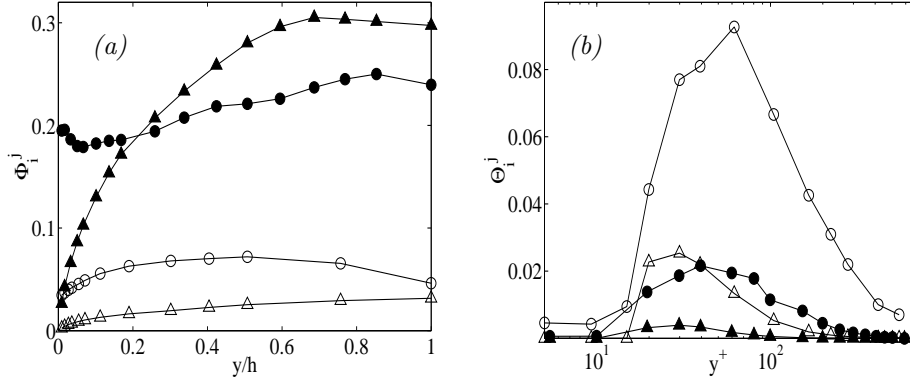


Figure 2: (a) Ratio Φ_i^j between the unresolved and total energies for the (i) velocity component along the direction (j), as a function of y . \circ , Φ_u^x ; \triangle , Φ_w^z . (b) Fraction Θ_i^j of the energy of the derivative of the (i) velocity component with respect to the direction (j), which is aliased along that same direction, plotted as a function of y . \circ , Θ_u^x ; \triangle , Θ_w^z . In all cases, the open symbols refer to the present $Re_\tau = 550$ simulation, and the closed ones to the one by [Moser, Kim & Mansour (1999)] at $Re_\tau = 590$.

the fractions Θ_v^x and Θ_u^z of the enstrophy contained in these underresolved tails in a way similar to Fig. 2(a). The underresolved enstrophy is in this case defined as the integral of the ‘hook’ in the premultiplied spectrum of the derivative in question, from the highest wavenumber to the location of its first minimum. There is more or less five times more underresolved enstrophy in our numerical channel than in the one from [Moser, Kim & Mansour (1999)]. The comparison of Figs. 2(a) and 2(b) shows that the improperly resolved enstrophy at the short-wave ends of the spectra is of the same order as that of the improperly resolved energy in their long-wave ends.

To achieve stationary statistics for structures of wavelength λ the simulation has to be run for several turnover times λ/u_τ , which becomes fairly expensive in these long boxes. Our experience with test cases at $Re_\tau = 180$ indicates that to have some confidence in the statistics of the largest scales the simulation should be run for roughly 10 wash-out times L_x/U_b , where U_b is the bulk mean velocity of the flow. The statistics presented here for the $Re_\tau = 550$ case have been collected during 10 wash-out times, after discarding initial transients.

3 Results

3.1 Two-dimensional velocity spectra in the near-wall region

Figs. 3 and 4 display linearly spaced isocontours of the premultiplied two-dimensional energy spectra $\phi_{ij} = k_x k_z E_{ij}(\lambda_x, \lambda_z, y)$ as functions of the wavelength vector $(\lambda_x, \lambda_z) = (2\pi/k_x, 2\pi/k_z)$. Note that

$$\langle u'_i u'_j \rangle = \int_0^\infty \int_0^\infty \phi_{ij}(\lambda_x, \lambda_z, y) d(\log \lambda_x) d(\log \lambda_z), \quad (1)$$

so that these figures express how much energy is contained in structures of length λ_x and width λ_z . The shaded contours come from the simulation at $Re_\tau = 550$, while the line contours are from the one at $Re_\tau = 180$. The four wall distances in Fig. 3 are $y^+ = 15$, $y^+ = 90$, $y = 0.2h$, $y = 0.5h$, corresponding respectively to the bottom and the top of the buffer layer, and the bottom and the core of the outer region. In Fig. 4 the three wall distances are $y^+ = 15$, $y^+ = 90$ and $y = 0.5h$.

In the wall region the spectrum of the streamwise velocity (Fig. 3a) peaks around $\lambda_x^+ \approx 700$, $\lambda_z^+ \approx 100$, which is the size of the buffer layer streaks. The spectra of the two other velocity components peak around $\lambda_x^+ \approx 250$, $\lambda_z^+ \approx 50 - 100$ (see Figs. 4a and 4b), corresponding approximately to the dimensions of an individual system of counterrotating quasi-streamwise vortices (Kim, Moin & Moser, 1987).

There is still not general agreement about the scaling in the near-wall region. Contrary to the classical idea that inner scaling should work close enough to the wall, several experimentalists have found evidence suggesting that this is not so, and in particular that the streamwise normal stress $\langle u'^2 \rangle$ increases with the

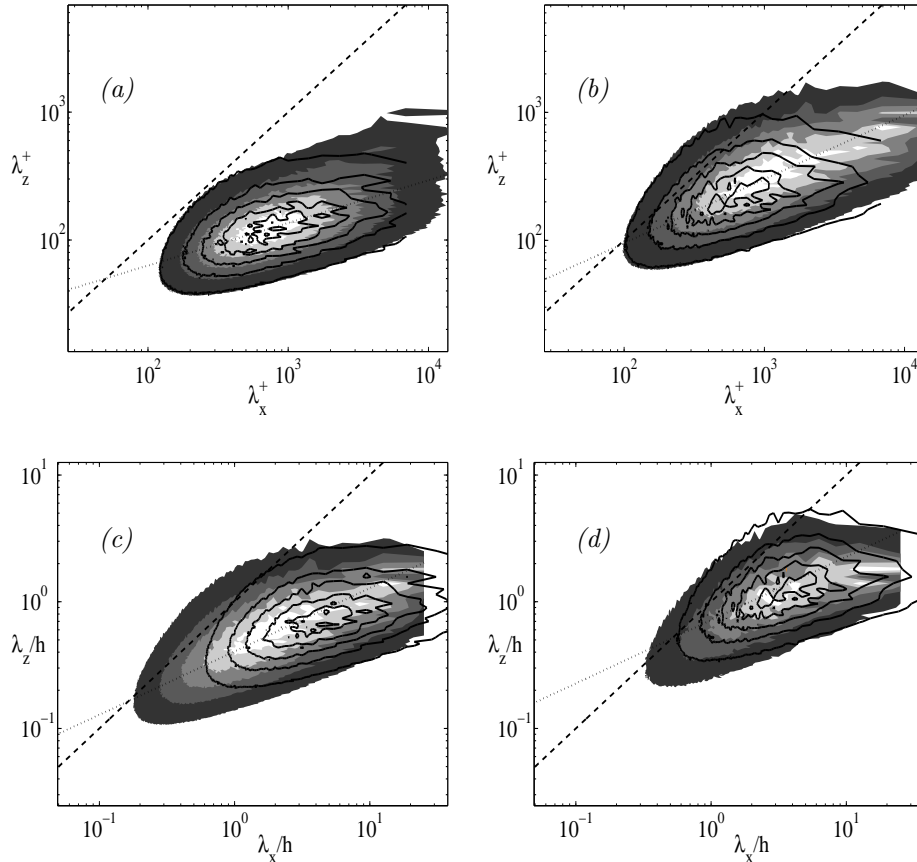


Figure 3: Premultiplied two-dimensional spectra ϕ_{uu} of the streamwise velocity, as functions of the streamwise and spanwise wavelengths at three representative wall distances. (a) Wall units, $y^+ = 15$; (b) Wall units, $y^+ = 90$ ($y = 0.5h$ at $Re_\tau = 180$); (c) Outer units, $y = 0.2h$ ($y^+ = 90$ at $Re_\tau = 550$); (d) Outer units, $y = 0.5h$. Shaded contours, $Re_\tau = 550$; line contours, $Re_\tau = 180$. In all the cases there are five linearly increasing contours. \cdots , locus of two-dimensional isotropic structures $\lambda_z = \lambda_x$; the dotted line in (a) is $\lambda_x^+ \sim (\lambda_z^+)^3$, passing through $\lambda_x^+ = \lambda_z^+ = 50$; those in (b), (c) and (d) are $\lambda_x y = \lambda_z^2$, and the point where this line crosses the dashed one corresponds to three-dimensionally isotropic structures.

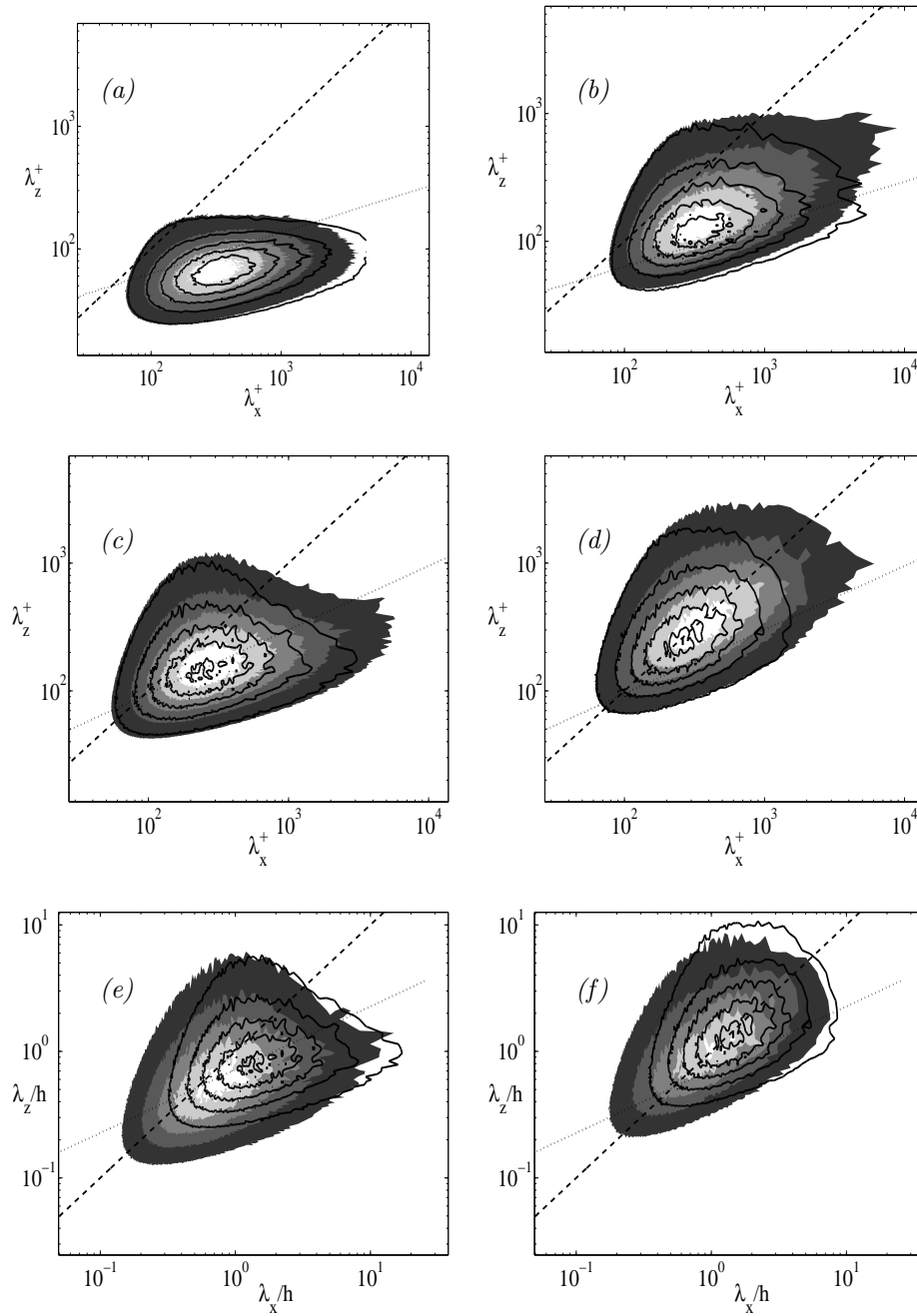


Figure 4: Premultiplied two-dimensional spectra as functions of the streamwise and spanwise wavelengths at three representative wall distances. (a), (c) (e), ϕ_{vv} ; (b), (d) (f), ϕ_{wv} . (a), (b) Wall units, $y^+ = 15$; (c), (d) Wall units, $y^+ = 90$ ($y = 0.5h$ at $Re_\tau = 180$); (e), (f) Outer units, $y = 0.5h$. Shaded contours, $Re_\tau = 550$; line contours, $Re_\tau = 180$. In all the cases there are five linearly increasing contours. \cdots , locus of two-dimensional isotropic structures $\lambda_z = \lambda_x$; the dotted lines in (a) and (b), are $\lambda_x^+ \sim (\lambda_z^+)^3$ passing through $\lambda_x^+ = \lambda_z^+ = 50$; those in (c), (d), (e) and (f) are $\lambda_x y = \lambda_z^2$ and the point where both lines cross in those figures corresponds to three-dimensionally isotropic structures.

Reynolds number throughout the wall layer, when expressed in wall units at a fixed y^+ . Some of these researchers (DeGraaf & Eaton, 2000; Perry & Li, 1990) have argued that the Reynolds number dependence is due to the contribution of Townsend’s (1976) ‘inactive’ motions. They note that this contribution scales in outer units, and are motivated by this observation to introduce ‘mixed’ scaling in which $\langle u'^2 \rangle$ is proportional to the geometric mean of the friction and outer velocities. [Hites (1997)] presents a similar argument, but favors an interpretation in which the inner and outer contributions are scaled independently, with no simple overall law. [Jiménez, Flores & García-Villalba (2001)], using data from [Hites (1997)] and from the present numerical simulations show that the short-wavelength end of the one-dimensional streamwise u spectrum at $y^+ = 20$ scales well in inner units, while its long-wavelength end scales in outer units. It was already noted by [Townsend (1976)] that the no-slip impermeability condition at the wall does not limit the size of the u and w velocity structures, while the effect of the no-slip condition is limited in height to a few wall units. We can therefore expect the large scales, even if they originate far from the wall, to penetrate deep into the near-wall layer, causing $\langle u'^2 \rangle$ to have both local and global contributions.

In fact, the only region of the two-dimensional u -spectra in Fig. 3(a) that does not collapse well in wall units is the upper-right corner, which corresponds to the large structures which dominate the outer-layer spectra in Figs. 3(c) and 3(d). As we move deeper into the buffer layer the energy contained in the large scales increases (Fig. 3b), in agreement with the common observation that the collapse of $\langle u'^2 \rangle$ in inner scaling worsens as the wall distance increases. Recent experimental spectra by [Metzger & Klewicki (2001)] at $y^+ = 15$ in the atmospheric boundary layer show that a substantial fraction of the streamwise turbulent energy is contained in very large structures at those extremely high Reynolds numbers ($Re_\theta \sim 10^6$). [Jiménez, Flores & García-Villalba (2001)] have argued that the effect is actually repressing, with the outer large scales preventing the wall streaks from becoming ‘infinitely’ long.

It is worth pointing out that the u spectrum in this region lies approximately along the power law

$$\lambda_x^+ \sim (\lambda_z^+)^3, \quad (2)$$

implying that, while the structures of the streamwise velocity become wider as they become longer, they also become more elongated, since they progressively separate from the spectral locus of two-dimensional isotropy. The spectrum of w does not share this property and is more isotropic in the (x, z) plane. The spectrum of v is very anisotropic in the near-wall region, but as we move away from the wall it develops a second isotropic component (Fig. 4c,e) whose relative strength increases with the wall distance, and which becomes dominant close to the center of the channel.

3.2 The very large anisotropic scales in the outer layer

Above $y^+ \approx 60$, the spectrum of the streamwise velocity becomes quite different from the spectra of the wall-normal and spanwise velocities, as we can see in Figs. 3 and 4. The spectrum of u is anisotropic and has two components. The first one is associated to small scales, and collapses fairly well for our two Reynolds numbers when plotted as a function of $(\lambda_x^+, \lambda_z^+)$ at a constant y^+ (Figs. 3*a* and 3*b*). The second one is related to large anisotropic structures and collapses well when plotted at a constant y/h as a function of $(\lambda_x/h, \lambda_z/h)$ (Figs. 3*c* and 3*d*). Below $y^+ \approx 60$ the small-scale component is the most important one, and the peak of the spectrum collapses in wall units as in Fig. 3*a*). Far from the wall ($y \gtrsim 0.3h$), it is the large-scale component which dominates, and the peak of the spectrum collapses in outer units as in Fig. 3*d*). This description suggests that, at least in turbulent channels at moderate Reynolds numbers, there exists a family of u structures in the inner region which scales in wall units and another one in the outer region which scales in outer units.

The present results resemble those of the high-Reynolds number experiments of [Hites (1997)] and [Kim & Adrian (1999)], although there is a significant difference. In the numerical channels the two spectral peaks corresponding to the VLAS and the wall streaks never coexist. Instead, we observe an intermediate region of wall distances ($y^+ \gtrsim 60, y \lesssim 0.3h$) where the peaks of the u spectra do not collapse in inner or in outer units (Figs. 3*c* and 3*d*). One reason for this discrepancy may be that the viscous and the large-scale components of the u spectra have comparable intensities in our moderate-Reynolds number simulations. [Hunt & Morrison (2000)] have noted that the energy contained in the outer structures increases with the Reynolds number and will eventually become much larger than that in the inner ones, so that the large scales would eventually become dominant even very near the wall. The failure to observe an overlap in our simulations could be related to that effect; although we clearly observe the two spectral components in the two-dimensional spectra, the outer one is never strong enough in the inner region to appear as a peak in the one-dimensional spectra. On the other hand, new measurements at extremely high Reynolds numbers by [Morrison *et al.* (2001)] in pipes do not show any region in the flow with double spectral peaks for the one-dimensional u -spectra, and the question should therefore be considered as still open.

The spectra of v and w are also in this region more isotropic than those of u . The spectrum for w is closer to two-dimensional isotropy than that of v , but it is flatter, in the sense that it is both wider and longer than v for a given height. It is difficult from the present results to obtain clear spectral scaling laws for the transverse velocity components. In the lower part of the outer layer the small scales of the spectra collapse well in inner units (Figs. 4*c* and 4*d*), similarly to what happens with the streamwise velocity, but in this case the large scales do not collapse in outer units. Further away from the wall we have been unable to find any scaling that collapses the spectra at $Re_\tau = 180$ with those at $Re_\tau = 550$. In Figs. 4*e*) and 4*f*) the spectra are represented in outer units and only collapse, and even then imperfectly, for the largest scales.

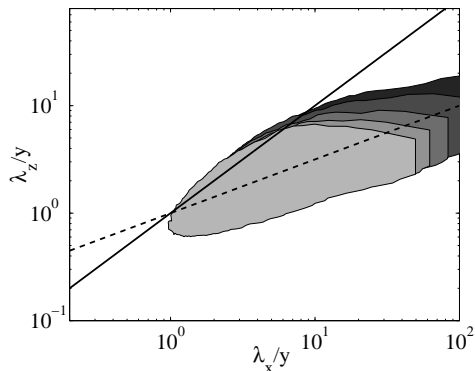


Figure 5: Superimposed contours of 0.2 times the maximum of ϕ_{uu} at five wall distances in the outer layer (from dark to light $y = 0.1h(0.1h)0.5h$). They are represented as functions of the streamwise and spanwise wavenumbers nondimensionalized with the wall distance. —, locus of two-dimensional isotropic structures $\lambda_z/y = \lambda_x/y$; \cdots , $(\lambda_z/y)^2 = \lambda_x/y$. The point where both lines cross corresponds to three-dimensionally isotropic structures.

The two-dimensional spectrum of the streamwise velocity exhibits a different behavior in the outer layer than in the wall region (see Eq. 2). Fig. 5 displays superimposed contours of ϕ_{uu} at five different wall distances in the outer layer ranging from $y = 0.1h$ (light) to $y = 0.5h$ (dark). The spectra are nondimensionalized with y and collapses well along the dashed line, which corresponds to the power law

$$\lambda_x y = \lambda_z^2. \quad (3)$$

A possible explanation for this power law is that the structures in the streamwise velocity are the decaying wakes of approximately isotropic v and w structures. Those of diameter λ_z decay in times of order λ_z^2/ν_T under the action of an eddy viscosity ν_T , leaving ‘wakes’ in the streamwise velocity whose length is

$$\lambda_x \sim U_b \lambda_z^2 / \nu_T, \quad (4)$$

assuming that they are convected at a velocity of the order of the bulk velocity. The choice of a constant advection velocity implies that necessarily the large structures feel the wall, since velocity itself is not a Galilean invariant.

The relation (3) not only expresses how ϕ_{uu} is organized in the plane (λ_x, λ_z) at a given wall distance. Since Eq. (4) links the coefficient of the power law in Eq. (3) to the magnitude of the eddy viscosity, the fact that all the spectra in Fig. 5 are aligned along a single line implies that ν_T is proportional to y , in agreement, and in strong support, to the similarity arguments about the scaling of the Reynolds stresses used in the standard derivations of the logarithmic velocity profile. It also helps understand why the outer structures become more isotropic with wall distance (which can be noticed from the displacement

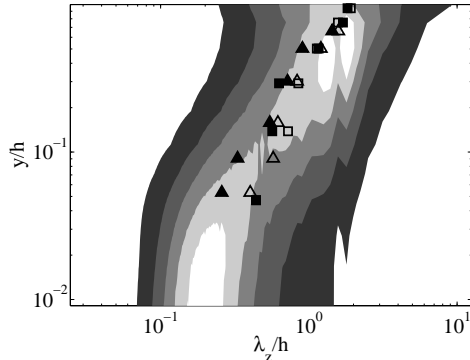


Figure 6: Premultiplied 1-D spectrum of streamwise velocity, in outer units. The shaded contours are the present $Re_\tau = 550$ simulation; the symbols are experiments by [Nakagawa & Nezu (1981)]. \blacktriangle and \triangle , $Re_\tau = 696$; \blacksquare and \square , $Re_\tau = 318$. Open symbols, $\langle \lambda \rangle_s$; closed symbols, $\langle \lambda \rangle_e$.

of the contours in figure 5), since the decaying time of the wakes decreases as the eddy viscosity increases. It should however be noted that the eddy viscosity in this flow, as measured from the mean velocity profile, only increases approximately linearly up to $y \approx 0.2$, and is constant thereafter, so that most of the spectra in Fig. 5 are outside the region of linear dependence. The present model can therefore only be taken as indicative until detailed calculations are carried out using the real eddy viscosity distribution. How it can be reconciled with the different power law (2) observed near the wall is briefly discussed in [Jiménez, Flores & García-Villalba (2001)].

The spectra of the three velocity components suggest that the u structures in the outer flow region resemble the buffer layer streaks, although they differ from them in that they are themselves turbulent, and in that it is unclear whether they are flanked by quasi-streamwise vortices. They seem however to be associated with roughly isotropic turbulent structures of the transverse velocities whose width increases with y (Fig. 4), but whose kinematics are unknown. The u -VLAS also widen with wall distance, specially above the buffer layer. This is shown in Fig. 6, which displays the transverse one-dimensional spectrum $k_z E_{uu}^{1D}$ at $Re_\tau = 550$. The spectrum has been plotted as a function of λ_z and y , and it has been non-dimensionalized with the local streamwise energy $\langle u^2 \rangle(y)$. The figure therefore shows how much energy is associated to u structures of a certain width λ_z at a given distance to the wall. The figure also includes the widths of the u structures obtained by [Nakagawa & Nezu (1981)]. They measured the spanwise organization in a turbulent open channel with a free surface using the autocorrelation of the streamwise velocity conditionally averaged with the presence of ejections, $\langle \lambda \rangle_e$, and sweeps, $\langle \lambda \rangle_s$. Their data agree reasonably well with ours even in the outer region, where the different

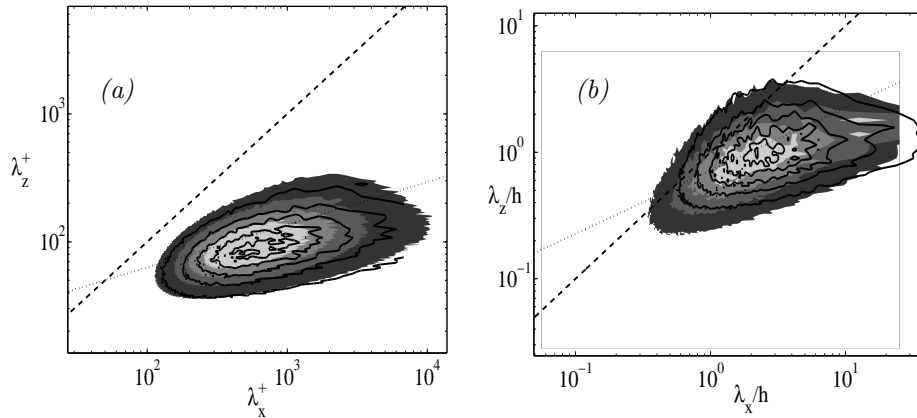


Figure 7: Premultiplied two-dimensional cospectra as functions of the stream-wise and spanwise wavelengths at two representative wall distances. (a) Wall units, $y^+ = 15$; (b) Outer units, $y = 0.5h$. Shaded contours, $Re_\tau = 550$; line contours, $Re_\tau = 180$. In all the cases there are five linearly increasing contours. \cdots , locus of two-dimensional isotropic structures $\lambda_z = \lambda_x$; the dotted line in (a) is $\lambda_z^+ \sim (\lambda_x^+)^3$, passing through $\lambda_x^+ = \lambda_z^+ = 50$; that in (b) is $\lambda_x y = \lambda_z^2$.

geometrical configurations could be expected to affect the nature of the flow. The transverse one-dimensional spectra of the transverse velocity components, not shown here, behave with y very much like those of u .

3.3 The cospectrum

The cospectrum is particularly important because its integral is the Reynolds stress $\langle u'v' \rangle$, and determines the mean velocity profile U and the production of turbulent kinetic energy.

Fig. 7 shows the premultiplied two-dimensional cospectra in the near-wall and in the outer regions of the flow in the same fashion as the two-dimensional premultiplied velocity spectra. They resemble much more the premultiplied spectra of u in Figs. 3(a) and 3(d) than those of v in Figs. 4(a) and 4(e). This is true at all wall distances. The cospectra collapse in inner scaling in the near-wall region and in outer scaling in the outer region, in the same way as the u -spectra. But unlike the latter the cospectra fully collapse in wall units in the near-wall region, suggesting that the outer large structures do not affect the Reynolds stresses very close to the wall. This result agrees with the experiments by [DeGraaff & Eaton (2000)], who found that $\langle u'v' \rangle$ scales in inner units close to the wall and give support to the law of the wall $U^+ = U^+(y^+)$. [Jiménez (1998)] also noted that the one-dimensional experimental cospectra in the logarithmic layer scaled with y much better than any of the other available velocity components.

It is of special interest that in the outer region, the VLAS carry a substantial fraction of the Reynolds stresses even if they are not present in the spectra of the wall-normal velocity in Fig. 4(e). [Jiménez (1998)] observed that the vanishing of the *premultiplied* spectrum of v for long or for wide waves is not sufficient to imply that the *premultiplied* cospectrum also vanishes in that limit, as it had been previously assumed (Perry, Henbest & Chong, 1986). Let

$$E_{uv} = \sigma_{uv}(E_{uu}E_{vv})^{1/2}, \quad (5)$$

where σ_{uv} is the structure parameter, which measures the correlation between u and v and the efficiency of those fluctuations in transporting momentum. In the present simulations, E_{vv} is independent of λ_x for the long scales and consequently, the premultiplied v spectrum

$$\frac{(2\pi)^2 E_{vv}}{\lambda_x \lambda_z},$$

goes to zero as $1/\lambda_x$ when $\lambda_x \gg 1$, while ϕ_{uu} decays more slowly. It then follows from the square root in in Eq. (5) that in the limit of very long wavelengths the behavior of the premultiplied cospectrum depends on the prefactor σ_{uv} .

Fig. 8 displays the spectral distribution of the structure parameter in the near-wall region and in the outer layer. Its magnitude is low around $\lambda_x = \lambda_z$, where it is approximately a function of the distance to that line, in agreement with the intuitive idea that isotropic turbulence cannot transport momentum. On the other hand, σ_{uv} approaches unity for the VLAS, which are thus shown to be very efficient in transporting momentum. The result is that they actually carry an important fraction of the Reynolds stresses in the outer flow, as shown in Fig. 7.

4 Discussion and conclusions

We have performed the first direct numerical simulation of turbulent channel flow using both a computational domain big enough to capture the largest structures in the outer flow and a Reynolds number high enough to observe some separation between those structures and the ones in the near-wall region.

The results show that there are very large elongated structures in the outer region of turbulent channel flow whose size scales with h . We have suggested that they can be understood as the wakes left by compact isotropic structures decaying under the action of an eddy viscosity as they are convected by the mean flow. Both the spectra and flow visualization suggest that the VLAS are also very high, and that they can hit the walls, which would help understand the Reynolds number dependence in the scaling of $\langle u'^2 \rangle$ in the near-wall region (Perry & Li, 1990; DeGraaf & Eaton, 2000). We have seen that the large structures in the outer layer widen with the wall distance faster than the buffer layer streaks, reaching widths of order of the channel height. The observed widening may be linked to the downstream evolution of the wakes that we have

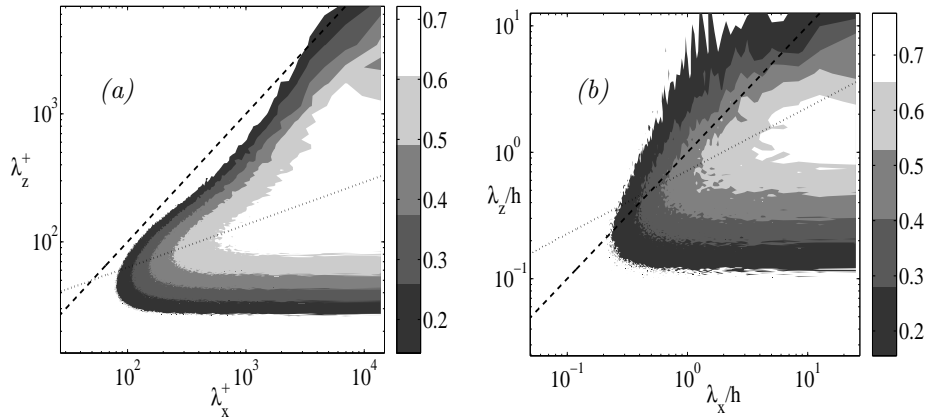


Figure 8: Structure parameter σ_{uv} as a function of the streamwise and spanwise wavelengths at two representative wall distances. Present $Re_\tau = 550$. (a) wall units, $y^+ = 15$; (b) outer units, $y = 0.5h$. In both cases there are five linearly increasing contours. \cdots , locus of two-dimensional isotropic structures $\lambda_z = \lambda_x$; the dotted line in (a) is $(\lambda_z^+)^3 \sim \lambda_x^+$ passing through $y^+ = 50$; that in (b) is $\lambda_z^2 = y\lambda_x$.

suggested as the origin of the VLAS. The large anisotropic structures in the outer flow not only carry a substantial fraction of the kinetic energy of the flow, but also a substantial fraction of the Reynolds stresses, and are therefore ‘active’ in the sense of [Townsend (1976)].

We have noted that our Reynolds number is still too low to draw strong scaling conclusions for some of the variables involved, because the separation between the outer and inner scales of the flow is still moderate. Computer limitations do not allow direct numerical simulations in the range of Reynolds numbers in [Hites (1997)], [Kim & Adrian (1999)], [Metzger & Klewicki (2001)] and [Morrison *et al.* (2001)] in a near future, although some of the open questions can probably be addressed at much lower Reynolds numbers. Large eddy simulations could be very valuable in this respect if they could be shown to represent the VLAS sufficiently well. The wake model that we have proposed suggests that they should, but it is still not sufficiently clear what is the origin of the forcing of those wakes, and whether they are independent of the detailed dynamics of the wall, which is imperfectly resolved by the LES.

This work was supported in part by the Spanish CICYT contract BFM2000-1468 and by ONR grant N0014-00-1-01416. We are specially indebted to the CEPBA/IBM center at Barcelona, and to IBM and the U. Politècnica de Catalunya, which have graciously donated the computer time needed for most of the simulations. Thanks are also due to R.D. Moser who reviewed a preliminary version of this manuscript.

References

- [Abe, Kawamura & Matsuo (2001)] ABE, H., KAWAMURA, H. & MATSUO, Y. 2001 Direct numerical simulation of fully developed turbulent channel flow with respect to the Reynolds number dependence. *J. Fluids Eng.* **123**, 382-393.
- [DeGraaff & Eaton (2000)] DEGRAAFF, D. B. & EATON, J. K. 2000 Reynolds-number scaling of the flat-plate turbulent boundary layer. *J. Fluid Mech.* **422**, 319-346.
- [Hites (1997)] HITES, M. H. 1997 Scaling of high-Reynolds number turbulent boundary layers in the National Diagnostic Facility. *Ph. D. Thesis*, Illinois Inst. of Technology.
- [Hunt & Morrison (2000)] HUNT, J.C.R. & MORRISON, J.F. 2000 Eddy structures in turbulent boundary layers. *Eur. J. Mech. B - Fluids* **19**, 673-694.
- [Jiménez (1998)] JIMÉNEZ, J. 1998 The largest structures in turbulent wall flows. *CTR Ann. Res. Briefs*, 943-945.
- [Jiménez, Flores & García-Villalba (2001)] JIMÉNEZ, J., FLORES, O. & GARCÍA-VILLALBA, M. 2001 The large scale organization of autonomous turbulent walls. *CTR Ann. Res. Briefs*, ??-??.
- [Kim & Adrian (1999)] KIM, K. C. & ADRIAN, R. J. 1999 Very large-scale motion in the outer layer. *Phys. Fluids A*. **11**, 417-422.
- [Kim, Moin & Moser (1987)] KIM, J., MOIN, P. & MOSER, R. D. 1987 Turbulence statistics in fully developed channel flow at low Reynolds number. *J. Fluid Mech.* **177**, 133-166.
- [Metzger & Klewicki (2001)] METZGER, M. M. & KLEWICKI, J. C. 2001 A comparative study of near-wall turbulence in high and low Reynolds number boundary layers. *Phys. Fluids A*. **13**, 692-701.
- [Morrison *et al.* (2001)] MORRISON, J.F., JIANG, W., MCKEON, B.J. & SMITS, A.J. 2001 Reynolds-number dependence of streamwise velocity spectra in turbulent pipe flow. *Submitted Phys. Rev. Lett.*
- [Moser, Kim & Mansour (1999)] MOSER, R. D., KIM, J. & MANSOUR, N. N. 1999 Direct numerical simulation of turbulent channel flow up to $Re_\tau = 590$. *Phys. Fluids A*. **11**, 943-945.
- [Nakagawa & Nezu (1981)] NAKAGAWA, H. & NEZU, I. 1981 Structure of space-time correlations of bursting phenomena in an open channel flow. *J. Fluid Mech.* **104**, 1-43.
- [Perry, Henbest & Chong (1986)] PERRY, A. E., HENBEST, S. & CHONG, M. S. 1986 A theoretical and experimental study of wall turbulence. *J. Fluid Mech.* **165**, 163-199.

- [Perry & Li (1990)] PERRY, A. E. & LI, J. D. 1990 Experimental support for the attached eddy hypothesis in zero pressure gradient boundary layers *J. Fluid Mech.* **218**, 405-438.
- [Smith (1994)] SMITH, R. W. 1988 Effect of Reynolds number on the structure of turbulent boundary layers *Ph. D. Thesis*, Department of Mechanical and Aerospace Engineering, Princeton University.
- [Townsend (1976)] TOWNSEND, A. A. 1976 *The structure of turbulent shear flows*, second ed., Cambridge U. Press.